GTFR 103

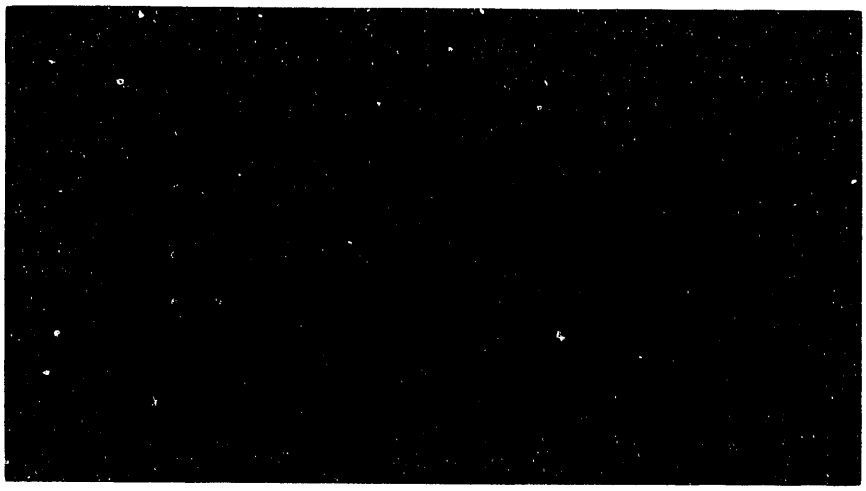

GEORGIA INSTITUTE OF TECHNOLOGY

Fusion Research Center
Georgia Institute of Technology
A Unit of the University System of Georgia
Atlanta, Georgia 30332

GTFR--103

DE93 002319

POLOIDAL ROTATION, DENSITY ASYMMETRIES AND MOMENTUM CONFINEMENT IN TOKAMAK EXPERIMENTS

W. M. Stacey
D. R. Jackson

Fusion Research Center
and
Nuclear Engineering Program
Georgia Institute of Technology
Atlanta, GA 30332 USA

August, 1992

DISCLAIMER

ABSTRACT

Poloidal rotation speeds and density asymmetries are calculated for the deuterium and dominant carbon (oxygen) impurity ions in discharges in ASDEX, DIII, ISX-B, JET and TFTR for which $v_\phi \sim v_{th}$ for the ions. These poloidal rotation speeds and density asymmetries are used to evaluate the neoclassical gyroviscous model for the momentum confinement time. The rather good agreement with experimental momentum confinement times obtained over this wide range of plasma parameters provides a measure of confidence in the calculated density asymmetries and poloidal rotation, as well as arguing for a neoclassical explanation for momentum confinement in tokamaks.

I INTRODUCTION

Poloidal asymmetries in ion density and poloidal bulk rotation of ions in the central regions of tokamak plasmas are related topics which are of intrinsic interest in the understanding of tokamak physics and which also are of importance to the interpretation of toroidal rotation experiments because they determine the magnitude of the neoclassical (gyroviscous) toroidal angular momentum transfer rate.[1] A calculational model was recently developed[2] which now allows the calculation of poloidal density asymmetries and poloidal rotation in tokamak plasmas with strong toroidal rotation ($v_\phi \sim v_{th}$).

The purposes of this paper are to apply the recently developed theory[2] to calculate the poloidal rotation and density asymmetries of the plasma and dominant impurity ions in a number of present and past tokamak experiments in which $v_\phi \sim v_{th}$ for the ion species and to compare the predictions of momentum confinement times evaluated with these rotation speeds and density asymmetries against experimental momentum confinement times. There are no good measurements of density asymmetries and poloidal rotation in the center of tokamak plasmas with which our predictions may be directly compared, but the comparison of momentum confinement times provides an indirect comparison with experiment.

We note that there is a great deal of interest in poloidal rotation in the plasma edge region in connection with L-H mode transition studies and that measurements of poloidal rotation speeds in the plasma edge region have been made.[3-5] The theory[2] that we use is ordered for $v_\phi \sim v_{th}$ and is thus not applicable to those measurements in which $v_\phi \sim \delta v_{th}$ and in which radial gradient terms that we order out must be retained.

The paper is organized as follows. The calculational models are briefly summarized in section II. The experimental parameters, the calculated poloidal rotation

and density asymmetries, and the comparison of theoretical and experimental momentum confinement times are described in section III. Related work is discussed in section IV. A summary is provided in section V.

II THEORY

A Poloidal Rotation and Density Asymmetries

The fluid theory[2] which we will use models NBI heated plasmas for which $v_\phi \sim v_{th}$ and $E/B_\theta \sim O(v_{th})$. Kinetic theory effects are accounted for in the viscosity and friction terms, following the Hirshman-Sigmar[6] moments approach.

The fluid particle equation

$$\nabla \cdot (n_j \mathbf{v}_j) = 0 \tag{1}$$

and the poloidal projection of the momentum balance equation

$$n_j m_j (\mathbf{v}_j \cdot \nabla) v_j + \nabla p_j + \nabla \cdot \overleftrightarrow{\pi}_j + e_j n_j \nabla \Phi - n_j e_j \mathbf{v}_j \times \mathbf{B} = \mathbf{R}_j + \mathbf{M}_j \tag{2}$$

were solved self-consistently in the large-aspect-ratio approximation to determine the poloidal velocity v_θ and density asymmetries $\tilde{n}^c$ and $\tilde{n}^s$ in tokamak plasmas.

In deriving the equations, the poloidal dependences were expanded in the form

$$x(r,\theta) = \bar{x}(r)[1 + \tilde{x}^s \sin\theta + \tilde{x}^c \cos\theta]. \tag{3}$$

The solution for the (normalized) poloidal velocity $\hat{v}_{j\theta}$ was obtained from the poloidal component of Eq. (2) by integrating over θ, and may be expressed in the form

$$\hat{v}_{j\theta} = \frac{driving}{damping} = \frac{driving}{viscosity + friction + inertia}. \tag{4}$$

In the above equation, *driving* (the driving force) is given by

$$\hat{M}_{j\theta} + \hat{v}_{jr} + \bar{\nu}^*_{jk}\sqrt{\frac{m_j}{m_k}}\hat{v}_{k\theta} - q^2\hat{v}^{ex2}_{j\phi}\left\{\frac{\tilde{\Phi}^s}{\epsilon} + \frac{\mathrm{f}_j}{2\hat{v}^{ex}_{j\phi}}\left[\frac{\tilde{\Phi}^s}{\epsilon}\frac{\tilde{n}^s_j}{\epsilon} + \frac{\tilde{\Phi}^c}{\epsilon}\left(5 + \frac{\tilde{n}^c_j}{\epsilon}\right)\right]\right\} \tag{5}$$

and the three *damping* terms are given by

$$\begin{aligned} viscosity \;\; &= \;\; q^2\mathrm{f}_j\left\{1 + \frac{5}{6}\frac{\tilde{n}^c_j}{\epsilon} + \frac{2}{3}\frac{\tilde{n}^s_j}{\epsilon} + \frac{1}{3}\left[\left(\frac{\tilde{n}^s_j}{\epsilon}\right)^2 + \left(\frac{\tilde{n}^c_j}{\epsilon}\right)^2\right]\right\} \\ &\quad + \frac{q^2\mathrm{f}_j}{2}\left\{\frac{\tilde{\Phi}^s}{\epsilon}\frac{\tilde{n}^s_j}{\epsilon} + \frac{\tilde{\Phi}^c}{\epsilon}\left(5 + \frac{\tilde{n}^c_j}{\epsilon}\right)\right\} \end{aligned} \tag{6}$$

$$friction = \bar{\nu}^*_{jk} \tag{7}$$

$$inertia = -q^2\hat{v}^{ex}_{j\phi}\left(\frac{\tilde{n}^s_j}{\epsilon} + \frac{\tilde{\Phi}^s}{\epsilon}\right). \tag{8}$$

We note that in the poloidal projection of the viscous stress tensor the parallel (η_0) component of the viscosity is the leading term and enters the above expression via terms containing f_j.

By taking the $\sin\theta$ and $\cos\theta$ moments of the poloidal component of Eq. (2), two equations (for each ion species) coupling $\tilde{n}^s_j$ and $\tilde{n}^c_j$ were obtained:

$$\left(\left(\frac{2}{3}f_j - \beta^2\bar{\nu}^*_{jk}\right)\hat{v}_{j\theta}\right)\frac{\tilde{n}^s_j}{\epsilon} - \frac{1}{2}\frac{\tilde{n}^c_j}{\epsilon} = -\left(\hat{v}^{ex}_{j\phi}\right)^2 + \frac{1}{2}\hat{\Phi}_j\frac{\tilde{\Phi}^c}{\epsilon} - \beta^2\bar{\nu}^*_{jk}\hat{v}_{j\theta}\frac{\tilde{n}^s_k}{\epsilon} \tag{9}$$

$$\begin{aligned} \left(\left(\frac{2}{3}f_j - \beta^2\bar{\nu}^*_{jk}\right)\hat{v}_{j\theta}\right)\frac{\tilde{n}^c_j}{\epsilon} + \frac{1}{2}\frac{\tilde{n}^s_j}{\epsilon} &= -f_j\hat{v}_{j\theta} - \frac{1}{2}\hat{\Phi}_j\frac{\tilde{\Phi}^s}{\epsilon} \\ &\quad + \beta^2\bar{\nu}^*_{jk}\left(\hat{v}_{j\theta} - \sqrt{\frac{m_j}{m_k}}\hat{v}_{k\theta}\right) - \beta^2\bar{\nu}^*_{jk}\hat{v}_{j\theta}\frac{\tilde{n}^c_k}{\epsilon} - \beta^2\hat{v}_{jr} \end{aligned} \tag{10}$$

Equations (4)–(10) are generally applicable to any number of ion species if $\bar{\nu}^*_{jk}$ is understood to represent a sum over species $k \neq j$. We specialize to the case of a main plasma species (j) and a dominant impurity species (k). Thus, Eqs. (4), (9), and (10) for each species constitute 6 coupled, nonlinear equations in the unknowns $\hat{v}_{j\theta}$, $\hat{v}_{k\theta}$, $\tilde{n}^s_j$, $\tilde{n}^s_k$, $\tilde{n}^c_j$, $\tilde{n}^c_k$ which must be solved numerically.

Some important dimensionless quantities which enter the above equations are defined as follows:

$$\epsilon \equiv \frac{r}{R} \qquad \bar{\nu}^*_{jk} \equiv \nu_{jk} qR/v_{thj} \qquad \beta \equiv B_\theta / B_\phi$$

$$f_j = \frac{\bar{\nu}^*_{jj}}{(\epsilon^{1.5} + \bar{\nu}^*_{jj})(1 + \bar{\nu}^*_{jj})} \qquad \hat{v}_{j\theta} \equiv \frac{\bar{v}_{j\theta}}{\beta v_{thj}} \qquad \hat{v}^{ex}_{j\phi} \equiv \frac{\bar{v}^{ex}_{j\phi}}{v_{thj}}$$

$$\hat{v}_{jr} \equiv \frac{\bar{v}_{jr}}{\beta \delta_j v_{thj}} \qquad \hat{M}_{j\theta} \equiv \frac{\hat{M}_{j\theta}}{\bar{n}_j m_j w_j v_{thj} \beta} \qquad \hat{\Phi}_j \equiv \frac{e_j}{\frac{1}{2} m_j} \frac{\bar{\Phi}}{v^2_{thj}} \tag{11}$$

where v_{thj} is the thermal speed, $\hat{v}_{j\theta}$, $\hat{v}^{ex}_{j\phi}$, and $\hat{v}_{jr}$ are the normalized poloidal, experimental toroidal, and radial velocities of ion species j, respectively, $\hat{M}_{j\theta}$ is the poloidal momentum input, $\hat{\Phi}_j$ is the normalized electrostatic potential, ν_{jk} is the collision frequency, q is the safety factor, and r and R are the minor and major radii.

B Momentum Confinement Time

The neoclassical (gyroviscous) momentum confinement time is[7]

$$\tau^{th}_\phi \equiv \frac{2\pi R \int_0^a \langle R n m v_\phi \rangle r dr}{2\pi R \int_0^a \langle R^2 \nabla\phi \cdot \nabla \cdot \overleftrightarrow{\pi}_j \rangle r dr} = \frac{2R^2 eB}{(\tilde{\Theta} G/Z)_{eff}} \frac{h_{nT_v}}{h_{nv}} \frac{\bar{m}_D}{m_D} \tag{12}$$

where

$$\left(\frac{\tilde{\Theta} G}{Z}\right)_{eff} \equiv \sum_{ions} \frac{\bar{n}_j}{\bar{n}_e} \tilde{\Theta}_j G_j. \tag{13}$$

The poloidal density asymmetry factor for each ion species is

$$\tilde{\Theta}_j \equiv (4 + \frac{\tilde{n}^c_j}{\epsilon})[-\hat{v}_{j\theta}(\hat{v}^{ex}_{j\phi})^{-1}(\frac{\tilde{\Phi}^s}{\epsilon} + \frac{\tilde{n}^s_j}{\epsilon}) + \frac{\tilde{\Phi}^s}{\epsilon}] + \frac{\tilde{n}^s_j}{\epsilon}[\hat{v}_{j\theta}(\hat{v}^{ex}_{j\phi})^{-1}(2 + \frac{\tilde{\Phi}^c}{\epsilon} + \frac{\tilde{n}^c_j}{\epsilon}) - \frac{\tilde{\Phi}^c}{\epsilon}] \tag{14}$$

where the $\tilde{\Phi}^{c/s}$ is related to the $\tilde{n}^{c/s}$ via charge neutrality and the electron momentum balance. When radial profiles have the form $(1 - (r/a)^2)^{\alpha_x}$, the radial profile factors have the form

$$G \equiv -\frac{r}{\eta_{4j} v_{\phi j}} \frac{\partial}{\partial r}(\eta_{4j} v_{\phi j}) = \frac{2(r/a)^2(\alpha_n + \alpha_v + \alpha_T)}{1 - (r/a)^2} \tag{15}$$

and

$$h_{nv} \equiv \frac{n(0)v_\phi(0)a^2}{2\int_0^a n(r)v_\phi(r)rdr} = 1 + \alpha_n + \alpha_v,\ etc. \tag{16}$$

The experimental momentum confinement may be written as[7]

$$\tau_\phi^{ex} = \frac{2\pi R\int_0^{\bar{a}}\langle Rnmv_\phi\rangle rdr}{\Gamma_\phi} = \frac{2\pi^2 a^2 R^2 n_{e0} m_D v_{\phi 0} h_{nv}^{-1}}{\Gamma_\phi} = \frac{2\pi^2 \bar{a}^2 R^3 n_{e0}\bar{m}_D \Omega_{\phi 0}^{ex}}{\Gamma_\phi h_{nv}} \tag{17}$$

where

$$\Gamma_\phi = \frac{\sqrt{2m_b}R_{tan}P_b}{\sqrt{E_b}} \tag{18}$$

is the torque input from NBI, R_{tan} is the tangency radius, E_b is the neutral beam energy, m_b is the mass of the beam particles, n_{e0} is the central electron density, $\Omega_{\phi 0}^{ex}$ is the central angular frequency, and $\bar{m}_D$ is an effective mass which reduces to m_D for deuterium plasmas.

III ANALYSIS OF EXPERIMENT

A Experimental Parameters

We reviewed the literature to identify at least one discharge for each of the major present and past tokamak experiments in which $v_\phi \sim v_{th}$ and for which the experimental parameters required to calculate both the poloidal speeds and density asymmetries and the momentum confinement times were available or could be reasonably extrapolated. We were able to identify such discharges for ASDEX, DIII, ISX-B, JET, and TFTR, which provides a wide range of experimental parameters. We elected to evaluate poloidal rotation and density asymmetries on a flux surface corresponding to r/a=0.5 and to use these values to evaluate the poloidal asymmetry factors, $\tilde{\Theta}$, that enter the calculation of momentum confinement times. Information concerning some input parameters was unavailable, however, and a few assumptions

were made and applied to all tokamaks: safety factor q(r/a=0.5)=2, since $q(0)\sim$ 1 and q(a)$\sim$ 3; $\beta = B_\theta/B_\phi = 0.1$; $e\Phi/T_i$=1; radial velocities $\hat{v}_{jr}$ and $\hat{v}_{kr}$=0; poloidal beam momentum inputs $\hat{M}_{\theta j}$ and $\hat{M}_{\theta k}$=0; radial profile of the form $x(r) = x_0(1-(r/a)^2)^{\alpha_x}$, except for DIII, where a density pedestal was included. The value of $e\Phi/T_i = 1$ was obtained for ISX-B[8] at a potential of 0.5 V and an average ion temperature of 500 eV. Since measurements of electrostatic potential were not available for the other machines, the value of $e\Phi/T_i$ obtained for ISX-B was assumed to be a reasonable estimate for all machines. The parameters that characterize the discharges analyzed in this paper are given in Table 1.

A well-documented[9,10] deuterium discharge with a dominant carbon impurity and with $\Omega_{\phi 0}$=9.1 $\times 10^4$ rad/s was analyzed for ASDEX. The peaking factors for density, angular velocity, and electron temperature[9]

$$Q_n = 1.6 \times (I_p/0.38)^{-0.35} \times (B_t/2.2)^{0.35}$$
$$Q_\Omega = 2.3 \times (I_p/0.38)^{-0.45} \times (B_t/2.2)^{0.95}$$
$$Q_{T_e} = 2.3 \times (I_p/0.38)^{-0.7} \times (B_t/2.2)^{0.7} \qquad (19)$$

where current has units of MA and magnetic field has units of T, were used to construct the profile parameters, α_x

$$Q_x \equiv \frac{x_0}{< x >} = 1 + \alpha_x. \qquad (20)$$

Due to the relatively high density in the case chosen for analysis, T_i and T_e were roughly equal.[10] Thus, the ion temperature profile factor α_T was assumed to be approximated by the electron temperature profile factor calculated from Q_{T_e}.

The data for DIII were obtained for deuterium plasmas with a dominant oxygen impurity. Data covering a wide range of experimental parameters were available.[11] However, experimental momentum confinement times were only available[12] for plasmas with somewhat different characteristics. The experimental parameters[11] were

Table 1: Summary of Machine and Plasma Parameters.

Machine	Ref.	Parameters												
		R (m)	$\bar{a}$ (m)	I_p (MA)	P_b (MW)	B_ϕ (T)	$v_\phi^{ex}(0)$ ($10^7 \frac{cm}{s}$)	$T_i(0)$ (keV)	$\frac{T_i}{T_e}$	$\bar{n_e}$ ($\frac{10^{13}}{cm^3}$)	z_{eff}	α_n	α_v	α_T
ASDEX	[9,10]	1.65	0.40	0.42	1.8	2.17	1.5	1.23	1.0	4.6	3.2	0.54	1.2	1.1
DIII	[11,12]	1.43	0.385	0.7	3.85	2.53	1.2	1.89	1.0	8.0	1.85	0.97	0.99	2.0
		1.44	0.38	0.71	6.1	2.53	1.6	2.23	0.97	8.0	2.0	0.96	1.1	1.9
ISX-B	[13–15]	0.93	0.25	0.155	0.85	1.4	1.1	7.16	1.0	4.5	2.5	1.0	1.0	1.0
JET (H)	[7,16]	3.00	1.10	3.1	7.7	2.2	2.0	5.5	1.25	3.0	2.3	0.0	1.5	1.5
JET (L)		3.00	1.10	3.22	14.25	3.47	3.5	15.5	1.5	1.33	3.5	2.0	3.0	3.5–4.0
TFTR	[17]	2.45	0.79	1.1	11.6	4.75	6.2	26.0	2.2	2.0	3.1	1.0	3.9	4.3

averaged over similar discharges and scaled to obtain parameters for two discharges for which momentum confinement data were available. The first case was an average of the data from two similar shots at a current of about 0.7 MA and 3.9 MW NBI. The other case was an average of the data from two similar shots at 0.71 MA and 6.1 MW NBI. The ion temperatures were scaled using the relation

$$T = T_1 \frac{P_b \tau_\phi n_{e1}}{P_{b1} \tau_{\phi 1} n_e} \tag{21}$$

where the subscript 1 indicates values at $\bar{n}_e = 8 \times 10^{13}$ cm^{-3}. The scaling was necessary since the plots of experimental confinement times[12] were available only for $\bar{n}_e = 8 \times 10^{13}$ cm^{-3}, whereas $\bar{n}_e$ for the tabulated data was lower. Straight-line fits to the plots of experimental confinement time versus beam power were not justifiable; τ_ϕ^{ex} varied slightly with P_b. The ratio of $P_b \tau_\phi$ to $P_{b1} \tau_{\phi 1}$ was set to unity in Eq. (21). The central velocities were available for only specific sets of data, namely P_b=3.7, 5.0, and 5.9 MW. The velocities at P_b=3.7 and 5.9 MW and a major radius of 1.52 m were chosen to describe the two cases at 3.9 and 6.1 MW (R$\sim$1.43 m). As mentioned, the density profile was parabolic-to-a-power plus a pedestal.

Analysis of ISX-B[13-15] began with determining the experimental toroidal velocity as a function of the neutral beam power. A straight-line fit to the data yielded

$$v_\phi = (8.5 + 2.4 P_b)(10^6) \tag{22}$$

with P_b in MW and v_ϕ in cm/s. In ISX-B, the study focused on hydrogen neutral beam co-injection in deuterium plasmas with a dominant carbon impurity. The central ion temperature for such a plasma is given by

$$T_i(0) = T_{OH}(0) + C \frac{P_b}{\bar{n}_e} \tag{23}$$

where C=2.2×10^{-19} keV $\cdot$ MW$^{-1} \cdot$ m^{-3} and $T_{OH}(0)$=0.3 keV. The experimental momentum confinement time was 17 ms at P_b=0.85 MW and $\bar{n}_e = 4.5 \times 10^{13}$ cm^{-3}. Using

these parameters in Eqs. (22) and (23) yields v_ϕ^{ex}=1.1×10^7 cm/s and T_{i0}=716 eV. Parabolic profiles were assumed.

Data for JET[7,16] covered both H-mode and L-mode deuterium plasmas with a dominant carbon impurity. For most H-mode discharges τ_ϕ^{ex}=200–500 ms, and for most L-mode discharges τ_ϕ^{ex}=100–200 ms.[7] However, ranges of experimental confinement times do not sufficiently indicate the accuracy of the theoretical model. For this reason, an experimental confinement time was constructed for one H-mode and one L-mode shot using the available data[16] and Eq. (17). Using an average R_{tan}=1.515 m (eight ion sources with R_{tan}=1.85 m and eight with R_{tan}=1.18 m),[7] the experimental momentum confinement time was 204 ms for the H-mode shot and 70 ms for the L-mode shot. Density profiles were flat in H-mode discharges and more peaked than parabolic in L-mode discharges. Velocity and temperature profiles varied from slightly more peaked than parabolic in H-mode discharges to parabolic to the fourth power in L-mode discharges. We chose representative profiles to be consistent with these observations.

A hot ion-mode discharge, which included temperature, velocity, and density profiles for a deuterium plasma with a carbon impurity, was chosen for the analysis of TFTR.[17] Determination of experimental momentum confinement time proceeded as for JET, with Γ_ϕ=18.25 N·m in Eq. (17), yielding an experimental momentum confinement time of 44 ms. Profile factors were determined from the measured profiles.

B Calculated Poloidal Rotation and Density Asymmetries

The calculated poloidal rotation speeds and density asymmetries are displayed in Table 2, and the dominant driving forces for these rotations and asymmetries are indicated in Table 3. The j and k subscripts denote deuterium and carbon (oxygen), respectively. $\hat{v}_{j\vartheta}$> 0 corresponds to rotation in the direction of the B_θ field, $\tilde{n}_j^s$> 0

Table 2: Poloidal Rotation and Density Asymmetries.

Machine	D $\hat{v}_{j\theta}$	C (O) $\hat{v}_{k\theta}$	D $\tilde{n}_j^c/\epsilon$	C (O) $\tilde{n}_k^c/\epsilon$	D $\tilde{n}_j^s/\epsilon$	C (O) $\tilde{n}_k^s/\epsilon$
ASDEX	-0.15	-0.35	0.064	0.38	0.0087	0.061
DIII (1)	-0.063	-0.17	0.057	0.45	0.011	0.040
DIII (2)	-0.11	-0.27	0.073	0.57	0.0073	0.12
ISX-B	-0.13	-0.32	0.075	0.46	0.030	0.037
JET (H)	-0.047	-0.073	0.035	0.21	-0.0049	0.045
JET (L)	-0.11	-0.075	0.028	0.17	-0.0056	0.024
TFTR	-0.12	-0.079	0.047	0.28	-0.0031	0.023

Table 3: Summary of Dominant Driving Forces.

Asymmetry		ASDEX,DIII,ISX-B	JET,TFTR
D	$\hat{v}_{j\theta}$	viscosity	viscosity,inertia
C (O)	$\hat{v}_{k\theta}$	viscosity,friction,inertia	viscosity
D	$\tilde{n}_j^s$	viscosity	E_θ
C (O)	$\tilde{n}_k^s$	viscosity	viscosity,inertia
D	$\tilde{n}_j^c$	inertia	inertia
C (O)	$\tilde{n}_k^c$	inertia	inertia

corresponds to an upward density shift, and $\tilde{n}_j^c > 0$ corresponds to an outward density shift—all in a right-hand (r, θ, ϕ) coordinate system in which the toroidal field and the toroidal current are aligned.

The density asymmetries, defined as

$$\tilde{n}(r) \equiv [n(r,\theta) - \bar{n}(r)]/[\bar{n}(r)], \tag{24}$$

are less than the inverse aspect ratio ϵ in all cases. While $\tilde{n}_k^c$ ranges from 0.17ϵ to 0.57ϵ, $\tilde{n}_j^c$ and $\tilde{n}_k^s$ are much smaller and range from 0.023ϵ to 0.12ϵ. The smallest density asymmetry is $\tilde{n}_j^s$, the magnitude of which is in the range 0.0031ϵ–0.03ϵ.

As the main ion and impurity ion species rotate in the toroidal direction (i.e.,

along the minor axis), inertial effects increase the density of the ions on the outboard side of the tokamak. Evaluation of each term coupling the density asymmetries showed that the largest term contributing to both $\tilde{n}_j^c$ and $\tilde{n}_k^c$ was indeed the inertia. The in-out density asymmetries are positive and increase with increasing values of the toroidal velocity, as would be expected. The inertial term also contributed to the up-down impurity density asymmetry for TFTR and JET, with $\tilde{n}_k^s$ increasing with increasing v_ϕ.

The viscosity, which is a function of the self-collision frequency, drove the impurity ion up-down asymmetry in ASDEX, DIII, and ISX-B. The up-down asymmetry for the main ion species in JET and TFTR was driven by a combination of factors acting to drive a poloidal electric field. The up-down density asymmetries for the main ion species in ASDEX, DIII, and ISX-B and for the impurity ion species in all devices show an upward shift. However, the main ion species are shifted downward in JET and TFTR.

Analysis of Eq. (4) showed that the viscosity terms drove the poloidal velocity in all cases. The dependence of the poloidal velocities on the viscosity was non-monotonic, a result which is consistent with the dependence of the quantity f on ν^* given by Eq. (11) and plotted in Fig. 1. The values of f, which determines the magnitude of the viscosity, for main deuterium ions and carbon (oxygen) ions is shown for the experiments in Fig. 1, with the leftmost value corresponding to the less collisional deuterium in each case. In general, the poloidal velocities were smallest for JET and TFTR. Furthermore, all values of v_θ were less than zero, indicating rotation opposite to the direction of B_θ for both species.

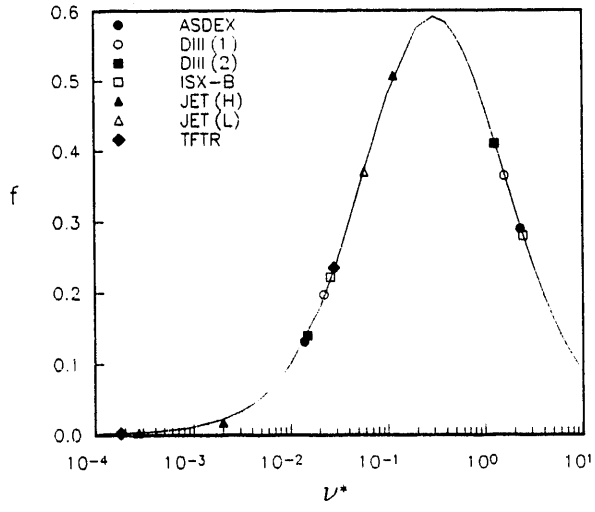

Figure 1: Viscosity as a Function of Self-collision Frequency.

C Comparison of Theoretical and Experimental Momentum Confinement Times

The poloidal rotation speeds and density asymmetries in Table 2 were used to evaluate the quantities $\tilde{\Theta}_j$ of Eq. (14) and the effective poloidal asymmetry factor defined by Eq. (13), the latter of which was used together with the experimental parameters given in Table 1 to evaluate the theoretical momentum confinement time from Eq. (12). The poloidal asymmetry factor so calculated was $\sim O(0.1)$, with the major contribution coming from the deuterium ions. The experimental momentum confinement time was either evaluated using the data from Table 1 in Eq. (17) or taken as quoted by the experimental team, as discussed in section III.A. The theoretical and experimental momentum confinement times are compared in Table 4 and Fig. 2. The rather good agreement provides some measure of confidence that the poloidal speeds and density asymmetries given in Table 2 are correct, albeit it does not constitute a

Table 4: Comparison of Theoretical and Experimental Momentum Confinement Times.

Machine	I_p (MA)	P_b (MW)	B_ϕ (T)	$v_\phi^{ex}(0)$ ($10^7 \frac{cm}{s}$)	$T_i(0)$ (keV)	$\bar{n}_e$ ($\frac{10^{13}}{cm^3}$)	τ_ϕ^{ex} ms	τ_ϕ^{th} ms
ASDEX	0.42	1.8	2.17	1.5	1.23	4.6	42	59
DIII	0.7	3.85	2.53	1.2	1.89	8.0	59	53
DIII	0.71	6.1	2.53	1.6	2.23	8.0	42	26
ISX-B	0.155	0.85	1.4	1.1	7.16	4.5	17	16
JET (H-mode)	3.1	7.7	2.2	2.0	5.5	3.0	204	240
JET (L-mode)	3.22	14.25	3.47	3.5	15.5	1.33	70	58–89
TFTR	1.1	11.6	4.75	6.2	26.0	2.0	44	50

direct confirmation.

We note that our calculation is a first-principles, neoclassical calculation. The relatively good agreement with experiment over a wide range of devices then argues for a neoclassical explanation of ion momentum transport in tokamaks.

IV RELATION TO OTHER WORK

There are literally no measurements of poloidal rotation or density asymmetries in the center of tokamak plasmas. As noted previously, there are several recent measurements[3–5,18] of poloidal rotation in the edge, but our ordering scheme ($v_\phi \sim v_{th}$) is generally not applicable. Up-down impurity density asymmetries have been measured[19–24] in the edge of several tokamaks; again our ordering scheme is generally not applicable.

A number of authors[22,25–27] have pointed out the contribution of friction and

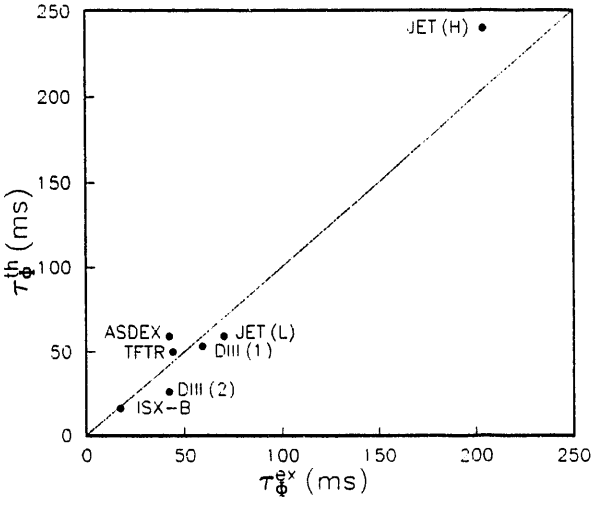

Figure 2: Comparison of Theoretical and Experimental Momentum Confinement Times.

inertia forces to driving asymmetries in the densities of very collisional ions. A self-consistent calculation[28,29] of toroidal and poloidal rotation and poloidal density asymmetries, similar to our model[2] but with a phenomenological representation of radial momentum transport instead of the neoclassical stress tensor, was made for ISX-B and PLT parameters some years ago. The deuterium poloidal rotation and density asymmetries obtained[29] are comparable to those given in Table 2 for ISX-B, but the high-Z impurity (titanium, tungsten) was calculated to have much larger poloidal rotation and density asymmetries than shown in Table 2 for carbon. This is consistent with the dependence of the calculation on collisionality reported previously.[2]

More recently, Kim et al.[30] have developed a neoclassical model for toroidal and poloidal rotation that is similar to the one[2] that we use. However, these authors do not treat the effect of poloidal density asymmetries on poloidal rotation, but do retain pressure gradient terms which order out in the $v_\phi \sim v_{th}$ ordering of our model.[2]

Variations of Eq. (12) have been used to rather successfully predict[7,12,17,31] momentum confinement times in a variety of tokamaks. Heretofore, the poloidal

asymmetry factor of Eq. (13), or some variant thereof, has been estimated instead of calculated. Our calculations of the poloidal asymmetry factors are quite close to the previously estimated values.

In a different vein, the calculations of this paper should resolve the controversy over neoclassical gyroviscous momentum transport, the salient remaining points of which we first summarize. Stacey and Sigmar[1] worked out the neoclassical stress tensor in toroidal coordinates and found that the gyroviscous contribution to the radial transport of toroidal angular momentum was proportional to the up-down asymmetry in toroidal velocity, which in turn depended on the up-down density asymmetry for the species in question. Based on their previous calculation[29] of $O(\epsilon)$ up-down density asymmetries for titanium/tungsten in ISX-B/PLT, they postulated that $O(\epsilon)$ up-down impurity density asymmetries could be present in tokamak experiments and showed that that alone (without regard for the deuterium density asymmetry) would make the gyroviscous momentum transport the proper magnitude to explain the experimentally observed momentum damping.

Connor et al.[32] analyzed Eqs. (1) and (2) and argued from ordering considerations that the poloidal rotation would, in essence, be 0.1δ times smaller than the thermal speed, where δ is the gyroradius-to-gradient-scale-length parameter. From this argument they concluded that the gyroviscous momentum transport would be orders of magnitude too small to explain the experimentally observed momentum damping rates. Stacey[33] then summarized evidence for $O(\epsilon)$ impurity asymmetries and pointed out an apparent inconsistency in the Connor et al. ordering argument when $v_\phi \sim v_{th}$.

Now that a first-principle, neoclassical calculation of the gyroviscous momentum damping rate has been performed, the "controversy" can be resolved. The model[2] used for the calculations of this paper is based on a consistent ordering when $v_\phi \sim v_{th}$.

Neoclassical theory predicts a (gyroviscous) momentum damping rate that is of the magnitude observed in tokamak experiments. This momentum damping is produced primarily by deuterium ion asymmetries of magnitude $<< O(\epsilon)$, rather than by $O(\epsilon)$ carbon or oxygen asymmetries as suggested by Stacey. The calculated poloidal rotation speeds are orders of magnitude larger than the values of 0.1δ times the thermal speed argued by Connor et al. purely on the basis of (apparently inconsistent) ordering considerations.

V SUMMARY

A recently developed neoclassical theory has been used to calculate the poloidal rotation and density asymmetries in ASDEX, DIII, ISX-B, JET, and TFTR. Using measured plasma parameters and a neoclassical model, the poloidal rotation velocity, the in-out density asymmetries, and the up-down density asymmetries were predicted for the hydrogenic and dominant carbon (oxygen) impurity species in these plasmas.

Adequate experimental data does not exist to allow a direct confirmation of the predictions. Thus, the validity of the theory was confirmed indirectly by comparing theoretical momentum confinement times, which depend directly on the poloidal velocities and density asymmetries, with the experimental momentum confinement times.

Analysis showed that the main ion and impurity ion poloidal velocities were in the negative B_θ direction and depended on the plasma viscosity and the inertial effects of the toroidal rotation. For more collisional impurities, the poloidal velocity was also affected by friction. The up-down density asymmetries for both ion species were affected mainly by a combination of the viscosity and the up-down potential asymmetries, while the in-out density asymmetries depended on the toroidal velocity

for both ion species. The magnitude of the poloidal rotation varied, for deuterium, from about $0.005v_{th}$ to $0.015v_{th}$ and, for carbon (oxygen) from about $0.007v_{th}$ to $0.035v_{th}$. The magnitude of the in-out density asymmetries varied, for deuterium, from about 0.03ϵ to 0.07ϵ and, for carbon (oxygen) from about 0.2ϵ to 0.6ϵ. The magnitude of the up-down density asymmetries varied, for deuterium, from about 0.003ϵ to 0.03ϵ and, for carbon (oxygen) from about 0.02ϵ to 0.1ϵ.

Using the calculated density asymmetries and poloidal rotation speeds to evaluate the poloidal asymmetry factors of the neoclassical gyroviscous theory, momentum confinement times were calculated which agreed with experimental values to within 6–40%. This level of agreement provides (indirectly) some confidence that the predicted density asymmetries and poloidal rotation speeds are correct and demonstrates that a first-principles neoclassical calculation can explain ion momentum confinement over a wide range of experimental parameters.

ACKNOWLEDGEMENTS

The calculations reported in this paper were performed as part of the M. S. Thesis[34] of one of the authors (DRJ), wherein greater detail may be found about the calculational procedures.

The authors thank Dr. A. Kallenbach for providing additional data essential to the analysis of the ASDEX rotation data.

This work was supported in part by the U. S. Department of Energy under the Grant DE-FG05-87ER51112 and in part by the Georgia Tech Fusion Research Center.

REFERENCES

[1] W. M. Stacey and D. J. Sigmar, *Phys. Fluids*, **28**, 2800 (1985).

[2] W. M. Stacey, "Poloidal rotation and density asymmetries in a tokamak plasma with strong toroidal rotation", Georgia Tech Report GTFR-101 (1992); *Physics of Fluids B*, to be published.

[3] R. J. Groebner, K. H. Burrell, and R. P. Seraydarian, *Phys. Rev. Lett.*, **64**, 3015 (1990).

[4] F. Wagner, F. Ryter, and A. R. Field et al., *Plasma Physics and Controlled Fusion Research–Proceedings of the 13th International Conference* (1991), Washington, IAEA (Vienna).

[5] Y. Miura, H. Aikawa, and K. Hoshino et al., *Plasma Physics and Controlled Fusion Research–Proceedings of the 13th International Conference* (1991), Washington, IAEA (Vienna).

[6] S. P. Hirshman and D. J. Sigmar, *Nucl. Fusion*, **21**, 1079 (1981).

[7] W. M. Stacey, *Nucl. Fusion*, **31**, 31 (1991).

[8] G. A. Hallock, J. Mathew, W. C. Jennings, and R. L. Hickock, *Phys. Rev. Lett.*, **56**, 1248 (1986).

[9] A. Kallenbach, H. M. Mayer, G. Fussmann, V. Mertens, U. Stroth, and O. Vollmer and the ASDEX Team, "Characterisation of the angular momentum transport in ASDEX", Report IPP I/255, Max-Planck-Institut für Plasmaphysik (October 1990).

[10] A. Kallenbach, Personal communication (July 1992).

[11] A. J. Groebner, W. Pfeiffer, F. P. Blau, K. H. Burrell, E. S. Fairbanks, R. P. Seraydarian, H. St. John, and R. E. Stockdale, *Nucl. Fusion*, **26**, 543 (1986).

[12] K. H. Burrell, R. J. Groebner, H. St. John, and R. P. Seraydarian, *Nucl. Fusion*, **28**, 3 (1988).

[13] R. C. Isler, L. E. Murray, E. C. Crume, C. E. Bush, J. L. Dunlap, P. H. Edmonds, S. Kasai, E. A. Lazarus, M. Murikami, G. H. Neilson, V. K. Pope, S. D. Scott, C. E. Thomas, and A. J. Wootton, *Nucl. Fusion*, **23**, 1017 (1983).

[14] R. C. Isler, A. J. Wootton, L. E. Murray, J. D. Bell, C. E. Bush, A. Carnevali, P. H. Edmonds, D. P. Hutchinson, R. R. Kindsfather, R. A. Langley, E. A. Lazarus, C. H. Ma, J. K. Munroe, M. Murikami, G. H. Neilson, S. D. Scott, and C. E. Thomas, *Nucl. Fusion*, **26**, 391 (1986).

[15] R. C. Isler and L. E. Murray, *Appl. Phys. Lett.*, **42**, 355 (1983).

[16] W. M. Stacey, *Nucl. Fusion*, **30**, 2453 (1990).

[17] G. Pautasso, Georgia Institute of Technology PhD Thesis (January 1992). Also W. M. Stacey, "Analysis of a dedicated rotation experiment in TFTR", Georgia Tech report GTFR-100 (1992). Copies may be ordered from National Technical Information Service, Springfield, VA 22161 as document no. PB92177187.

[18] K. Ida, S. Hidekuma, M. Kojima, Y. Miura, S. Tsuji, K. Hoshino, M. Mori, N. Suzuki, and T. Yamauchi, *Phys. Fluids B*, **4**, 2552 (1992).

[19] J. L. Terry, E. S. Marmar, K. I. Chen, and H. W. Moos, *Phys. Rev. Lett.*, **39**, 1615 (1977).

[20] S. L. Allen, H. W. Moos, R. K. Richards, J. L. Terry, and E. S. Marmar, *Nucl. Fusion*, **21**, 251 (1981).

[21] S. Suckewer et al., "Rapid scanning of spatial distribution of spectral line intensities in PLT tokamak", Princeton Plasma Physics Laboratory report PPPL-1430 (1978). Copies may be ordered from National Technical Information Service, Springfield, VA 22161 as document no. PPPL-1430.

[22] K. Brau, S. Suckewer, and S. K. Wong, *Nucl. Fusion*, **23**, 1657 (1983).

[23] P. Smeulders, *Nucl. Fusion*, **26**, 267 (1986).

[24] K. W. Wenzel, *Bull. Am. Phys. Soc.*, **34**, 2153 (1989).

[25] C. S. Chang and R. D. Hazeltine, *Nucl. Fusion*, **20**, 1397 (1980).

[26] K. H. Burrell, T. Ohkawa, and S. K. Wong, *Phys. Rev. Lett.*, **47**, 511 (1981).

[27] C. T. Hsu and D. J. Sigmar, *Plasma Phys. Contr. Fusion*, **32**, 499 (1990).

[28] W. M. Stacey and D. J. Sigmar, *Phys. Fluids*, **27**, 2076 (1984).

[29] W. M. Stacey, A. W. Bailey, D. J. Sigmar, and K. C. Shaing, *Nucl. Fusion*, **25**, 463 (1985).

[30] Y. B. Kim, P. H. Diamond, and R. J. Groebner, *Phys. Fluids B*, **3**, 2050 (1991).

[31] W. M. Stacey, C. M. Ryu, and M. A. Malik, *Nucl. Fusion*, **26**, 293 (1986).

[32] J. W. Connor, S. C. Cowley, R. J. Hastie, and L. R. Pan, *Plasma Phys. Contr. Fusion*, **29**, 919 (1987).

[33] W. M. Stacey, *Plasma Phys. Contr. Fusion*, **31**, 1451 (1989).

[34] D. R. Jackson, "A study of poloidal asymmetries in tokamaks", Georgia Institute of Technology Master's Thesis (1992).

APPENDIX: SOLUTION TO NONLINEAR EQUATIONS

The six nonlinear equations given by Eqs. (4), (9), and (10) were solved using HYBRID (created by B. S. Garbow, K. E. Hillstrom, and J. J. More at Argonne National Laboratory, 1980). HYBRID is a general nonlinear equation solver which finds the zeros of a system of n nonlinear equations in n unknowns. The system of equations is provided by the user in the form of a subroutine to HYBRID. Solution of the equations is calculated by the forward-difference approximation.

The subroutine included in this appendix was created by rewriting each of the six nonlinear equations with all terms on the left-hand-side of the equation such that the value of the right-hand-side was zero. The first execution of the subroutine resulted in an estimate of the roots of the system of nonlinear equations (using an initial guess of zero for each root). Subsequent calls to the subroutine yielded estimates of the roots until successive estimates varied by 10^{-5} or less for each root. The asymmetries thus calculated were used to calculate the normalized poloidal and radial profile factors, which in turn were used to calculate the theoretical momentum confinement time according to Eq. (12).

```
      subroutine fcn (n,x,fvec,iflag,istar,vthetaj,vthetak)

      integer n,iflag,istar,style
      double precision x(n),fvec(n),q,beta,rnukj,alpha,zj,rmk,
     *  rmj,rmjtheta,rmktheta,vjrad,vkrad,vphiex0,q2,vphiexk2,
     *  beta2,vphiexj2,ep,fj,fk,rnujk,phij,phik,c1,c2,c3,c4,c5,
     *  c6,phic,phis,thetaz,thetai,alphan,alphav,zk,
     *  vthetaj,vthetak,rnujj,rnukk,alphat,zeff,G,thetagz,rne0,
     *  ephiti,rmajor,rminor,temp0,bphi,hntv,hnv,rmd,rmdbar,rne,
     *  tauphi,rovera2,vphiexj,vphiexk,titote,rnebar,densrat,
     *  rnztone,rnitone
      character tok*40, inform*60

c  read in data on initial run
      if(istar.eq.1)then
        open(unit=1,file='xsecin')
        istar=2
        read(1,'(a40)')tok
        read(1,'(a60)')inform
        read(1,'(i3)')style
        read (1,*) rnukk, vjrad, vkrad, vphiex0, vphiexj, vphiexk
        write(2,'(" nuzzstar     vzrad        virad    vphiex0")')
        write(2,'(d10.3,3x,f6.3,6x,f6.3,6x,d10.3)')
     *  rnukk,vjrad,vkrad,vphiex0
        if(style.eq.3)then
            read (1,*) alpha, q, zeff, titote, densrat
        else
            read (1,*) alpha, q, zeff, titote
        endif
        write(2,*)
        write(2,'("alpha          q            zeff       Ti/Te")')
        write (2,5) alpha, q, zeff,titote
        read (1,*) zk, rmk, zj, rmj, beta
        write(2,*)
        write(2,'("zimp         massz          zion    massion")')
        write (2,5) zk, rmk, zj, rmj
        read (1,*) ephiti, rmjtheta, rmktheta, rnztone, rnitone
        write(2,*)
        write(2,'("e*phi/Ti        Mitheta     Mztheta")')
        write (2,5) ephiti, rmjtheta, rmktheta
5       format (4(f6.3,7x))
        read (1,*) alphan, alphav, alphat, rne0
        write(2,*)
```

```
        write(2,'("alphan        alphav        alphat     ne0")')
        write (2,15) alphan, alphav, alphat, rne0
15      format(3(f6.3,7x),d10.3)
        read (1,*) rovera2, rmajor, bphi, temp0, rnebar
        write(2,*)
        write(2,'("(r/a)^2     major radius    bphi       Tion(0)
     *nebar")')
        write (2,12) rovera2, rmajor, bphi, temp0, rnebar
12      format (f6.3,7x,f6.3,8x,f6.3,4x,f10.3,4x,d10.3)
        read (1,*) rmd, rmdbar, rne, rminor
        write(2,*)
        write(2,'("m sub D     m sub d bar    minor radius  ")')
        write (2,9) rmd, rmdbar, rminor
9       format (f6.3,8x,f6.3,7x,f6.3)
        read(1,*) rnujj, ep, fk, fj, rnujk, rnukj
        read(1,*) phij, phik
        read(1,*) c1, c2, c3, c4, c5, c6
        write(2,*)
        write(2,'("nuii star=",d10.3)')rnujj
        write(2,'("epsilon=",d10.3)')ep
        write(2,'("f ion and f impurity: ",2(d10.3))') fj, fk
       write(2,'("ion-impurity and impurity-ion collision freq: ",
      *    d10.3,3x,d10.3)')rnujk, rnukj
       write(2,'("phii hat and phiz hat:",d10.3,3x,d10.3)')
      *    phij,phik
        close(1)
        beta2=beta*beta
        q2=q*q
        vphiexj2=vphiexj*vphiexj
        vphiexk2=vphiexk*vphiexk
       endif
c  begin calculation of roots
       if(istar.eq.1 .or. istar.eq.2)then
c  potential asymmetries
       phic=(x(5)/c2+x(6)/c1)/(ephiti*titote)
       phis=(x(3)/c2+x(4)/c1)/(ephiti*titote)
c  user-supplied system of equations
       fvec(1)=x(1)*(q2*fj*(1.0d0 + 5.0d0*x(5)/6.0d0
      *        + 2.0d0*x(3)/3.0d0 + 1.0d0*x(3)*x(3)/3.0d0
      *        + 1.0d0*x(5)*x(5)/3.0d0 + phis*x(3)/2.0d0
      *        + 0.5d0*phic*(5.0d0+x(5))) + rnujk
      *        - q2*vphiexj*(x(3)+phis))
      *        - rmjtheta - vjrad - c5*x(2) + q2*vphiexj2
```

```
     *        * phis + 0.5d0*q2*fj*vphiexj*(phis*x(3)
     *        + phic*(5.0d0 + x(5)))

      fvec(2)=x(2)*(q2*fk*(1.0d0 + 5.0d0*x(6)/6.0d0
     *        + 2.0d0*x(4)/3.0d0 + 1.0d0*x(4)*x(4)/3.0d0
     *        + 1.0d0*x(6)*x(6)/3.0d0 + phis*x(4)/2.0d0
     *        + 0.5d0*phic*(5.0d0+x(6))) + rnukj
     *        - q2*vphiexk*(x(4)+phis))
     *        - rmktheta - vkrad - c6*x(1) + q2*vphiexk2
     *        * phis + 0.5d0*q2*fk*vphiexk*(phis*x(4)
     *        + phic*(5.0d0 + x(6)))

      fvec(3)=c3*x(1)*x(3) + vphiexj2 - 0.5d0*x(5)
     *        - 0.5d0*phij*phic + beta2*rnujk*x(1)*x(4)

      fvec(4)=c4*x(2)*x(4) + vphiexk2 - 0.5d0*x(6)
     *        - 0.5d0*phik*phic + beta2*rnukj*x(2)*x(3)

      fvec(5)=x(1)*c3*x(5) + x(1)*fj + 0.5d0*x(3) + 0.5d0*phij*phis
     *        - beta2*rnujk*x(1) + beta2*c5*x(2)
     *        + beta2*rnujk*x(1)*x(6) + beta2*vjrad

      fvec(6)=x(2)*c4*x(6) + x(2)*fk + 0.5d0*x(4) + 0.5d0*phik*phis
     *        - beta2*rnukj*x(2) + beta2*c6*x(1)
     *        + beta2*rnukj*x(2)*x(5) + beta2*vkrad
      endif
c  after solving equations, calculate confinement time
      if(istar.eq.3)then
          phic=(x(5)/c2+x(6)/c1)/(ephiti*titote)
          phis=(x(3)/c2+x(4)/c1)/(ephiti*titote)
          write(2,'("phic and phis: ",d10.3,3x,d10.3)') phic, phis
c  poloidal profile factors
          thetaz=(4.0d0+x(6))*((-x(2)*(phis+x(4))/vphiexk)
     *           + phis) + x(4)*((x(2)*(2.0d0+phic
     *           + x(6))/vphiexk) - phic)
          thetai=(4.0d0+x(5))*((-x(1)*(phis+x(3))/vphiexj)
     *           + phis) + x(3)*((x(1)*(2.0d0+phic
     *           + x(5))/vphiexj) - phic)
          write(2,'("theta z and theta ion: ",d10.3,3x,d10.3)')
     *    thetaz, thetai
c  radial profile factor for DIII
          if(style.eq.3)then
              G=2.0d0*rovera2*(alphan+alphav+alphat)*(1.0d0+densrat*
```

```
     *        ((alphat+alphav)*((1.0d0-rovera2)**(-alphan))/
     *        (alphan+alphat+alphav) - 1.0d0))/
     *        ((1.0d0-rovera2)*(1.0d0 + densrat*(((1.0d0-rovera2)**
     *        (-alphan)) - 1.0d0)))
c  radial profile factor for other tokamaks
          else
              G=2.0d0*rovera2*(alphan+alphav+alphat)/
     *        (1.0d0-rovera2)
          endif
          write(2,'("G: ",d10.3)') G
          thetagz=(rnztone*thetaz + rnitone*thetai)*G
          write(2,10)thetagz
10        format('(theta*G/z)eff = ',d10.3)
          hntv=1.0d0+alphan+alphat+alphav
          hnv=1.0d0+alphan+alphav
          rmajor2=rmajor*rmajor
c  theoretical momentum confinement time (msec):
c  major radius (rmajor) in meters, toroidal magnetic field
c  (bphi) in Tesla, central ion temperature (temp0) in electron
volts
c     DIII
          if(style.eq.3)then
             tauphi=2.0d3*rmajor2*bphi*(1.0d0+alphat/(1.0d0+
     *        alphan+alphav))*(1.0d0+densrat*alphan/(1.0d0+
     *        alphav))*rmdbar/
     *        (temp0*(1.0d0 +densrat*alphan/(1.0d0+alphav+
     *        alphat))*rmd*thetagz)
c      other tokamaks
          else
              tauphi=2.0d3*rmajor2*bphi*hntv*rmdbar/
     *              (temp0*hnv*rmd*thetagz)
          endif
          write(6,'(a40, "tauphi = ",f7.0)')tok,tauphi
          write(2,20)tauphi
20    format('theoretical momentum confinement time (msec)  =',
f9.2)
          write(2,*)
          write(2,*)
       endif

       return
       end
```

DATE
FILMED
01/20/93